Journal of Applied Polymer Science

Chemical modification of cashew gum with acrylamide using an ultrasound-assisted method

Jalma Maria Klein,[1] Vanessa Silva de Lima,[1] José Manoel Couto da Feira,[1] Rosmary Nichele Brandalise,[2] Maria Madalena de Camargo Forte[1]

[1]Laboratory of Polymeric Materials (LAPOL), Engineering School, Federal University of Rio Grande do Sul (UFRGS), P.O. Box 15010, Porto Alegre RS, 91501-970, Brazil

[2]Exact Science and Technology Center, University of Caxias do Sul (UCS), P.O. Box 1352, Caxias do Sul RS, 95070-560, Brazil

Correspondence to: M. M. C. Forte (E-mail: mmcforte@ufrgs.br)

ABSTRACT: A flocculant based on cashew gum (CG) grafted with polyacrylamide (PAM) was synthesized using potassium persulfate as the chemical initiator and ultrasound energy. The intrinsic viscosity, hydrodynamic radius, and grafting efficiency of the grafted copolymers (CG-*g*-PAM) were investigated at different monomer and initiator concentrations. The CG-*g*-PAM copolymers were evaluated in kaolin suspension and river water by using jar test procedure comparatively to a commercial flocculant (Flonex-9045). Ultrasonication resulted in reduced reaction time and high grafting efficiency. The reaction gel point was reached within 10 min and the grafting efficiency was dependent on the acrylamide concentration. The grafted copolymer CG-*g*-PAM-15^{285} obtained with 0.285 mmol of initiator showed higher hydrodynamic radius, with flocculation efficacy of 96% comparable with the flocculant Flonex-9045.
 J. Appl. Polym. Sci. **2016**, *133*, 43634.

KEYWORDS: copolymers; grafting; polyelectrolytes; polysaccharides

Received 26 September 2015; accepted 9 March 2016
DOI: 10.1002/app.43634

INTRODUCTION

Natural gums, in general, are one of the most abundant industrial raw materials and have been the subject of intensive research owing to their sustainability, biodegradability, and biosafety.[1,2] The gums are large polysaccharide molecules, consisting of multiple sugar units that are linked together and are available from renewable resources. Native gums are fairly shear stable, but have a poor shelf life because of uncontrollable rates of hydration and experience a drop in viscosity under storage.[3,4] To overcome their drawbacks, chemical modification of the polysaccharides is necessary to fine-tune their properties for a wide range of applications. The gums have been transformed into highly customizable materials with hybrid properties for different applications, such as drug delivery agents,[2,5] adhesives,[6] superabsorbent hydrogel,[7] and flocculants.[8–10] One of the most effective methods of chemical modification is the grafting of synthetic polymers onto the polysaccharide backbone.

A majority of grafting reactions have been performed via a conventional method involving free radical initiators.[7,11,12] Other methods involve the use of microwave energy[13,14] and high-energy radiation such as gamma rays[15] and electron beams,[16] in which active free radicals are generated by the thermal and photochemical dissociation of an initiator. Recently, ultrasound energy has also been used to generate free radicals from water-soluble initiator.[17–19] Sonochemistry-based methods are environmentally friendly and in line with the concept of 'Green Chemistry',[20] in addition to the ultrasound technology being a promising energy source for chemical reactions. The ultrasound effect comes from localized hot spots that are generated during the collapse of cavitation bubbles. Collapsing bubbles, which have a very short lifetime, produce intense localized heating (≈5000 K) and high pressure (≈1000 atm)[21] Ultrasound energy has been used in the hydrolysis and cleavage of di- and polysaccharides,[22] but rarely in chemical modification of polysaccharides. Some previous studies have focused on the use of ultrasound energy for the polymerization of alkyl methacrylates and styrene, and in experiments involving fuel cell materials.[19,23–25]

Flocculants based on modified polysaccharides for wastewater treatment are attractive, mainly for two reasons. Firstly, the possible link between Alzheimer's disease and residual aluminum in treated water, resulting from the use of inorganic coagulants such as alum and poly(aluminum chloride). Secondly, the risk of severe neurotoxic effects because of the presence of residual unreacted monomers, such as acrylamide, ethyleneimine, and trimethylolmelamine in synthetic organic flocculants.[26–28]

Table I. Reaction Conditions, Percentage of Grafting (%*G*), Grafting Efficiency (%*E*), Percentage of Conversion of Acrylamide (%*C*), Intrinsic Viscosity, and Hydrodynamic Radius of the Pristine CG, PAM Homopolymer, and CG-*g*-PAM Copolymers

Samples	Ratio Aam/CG[a]	KPS (mmol)	%*G*′	%*G*	%*E*	%*C*	Intrinsic viscosity (dL/g)	Hydrodynamic radius (nm)
CG								163
PAM[b]		0.190					3.49 ± 0.02	204
CG-*g*-PAM-6^{190}	6/1	0.190	50	99	55	38	2.22 ± 0.17	>250
CG-*g*-PAM-6^{285}		0.285	56	126	62	48	1.97 ± 0.20	>250
CG-*g*-PAM-6^{380}		0.380	64	183	71	59	1.28 ± 0.30	205
CG-*g*-PAM-10^{190}	10/1	0.190	78	348	84	80	1.63 ± 0.41	>250
CG-*g*-PAM-10^{285}		0.285	78	357	85	82	1.71 ± 0.32	>250
CG-*g*-PAM-10^{380}		0.380	78	355	85	81	1.17 ± 0.51	147
CG-*g*-PAM-15^{190}	15/1	0.190	86	615	94	94	1.56 ± 0.38	>250
CG-*g*-PAM-15^{285}		0.285	86	619	94	94	2.18 ± 0.18	>250
CG-*g*-PAM-15^{380}		0.380	86	612	93	93	2.31 ± 0.47	187
CG-*g*-PAM-20^{190}	20/1	0.190	89	778	90	89	3.67	NA
CG-*g*-PAM-control I[c]	15/1	0.285	83	495	79	75	8.25	NA
CG-*g*-PAM-control II[d]			83	481	77	73	5.10	NA

[a] CG = anhydroglucose unit (molar mass = 162 g).
[b] [Aam] = 2*M*.
[c,d] Control reactions carried out using thermostatic water bath at 56 °C for 30 min, and 70 °C for 13 min, respectively.
NA, Not analyzed.

We investigated the chemical modification of cashew gum (CG) with polyacrylamide (PAM) using potassium persulfate as the initiator and ultrasound energy, and the subsequent use of the modified CG as a flocculant. CG is a natural exudate of trees, from the species *Anacardium occidentale* L., which is widely cultivated in northeastern Brazil. CG is employed locally as a substitute for arabic gum in the pharmaceutical and cosmetic industries.[29] The composition of polysaccharide after hydrolysis consists of a high content of β-D-galactose (72%) and other side components such as glucose (14%), arabinose (4.6%), rhamnose (3.2%), and glucuronic acid (4.7%).[30] The aim of this work is to obtain a biodegradable PAM-based CG flocculant for water treatment. Such kind of flocculant has advantages over other commercial PAM-based flocculants owing to its biodegradable main chain, which is functionally grafted with long PAM chain branching. The use of grafted copolymers of CG with polyacrylamide (CG-*g*-PAM) eliminates the possible contamination of wastewater treatment sludge with acrylamide residual monomer, and circumvents the use of non-biodegradable polymeric flocculants, thereby reducing soil pollution in the long term. This study also sought to evaluate the use of ultrasound energy, instead of microwave, in facilitating grafting reactions at shorter reaction time compared to conventional methods.[31] Graft copolymers were synthesized at different monomer and initiator concentrations, and evaluated as a flocculant using kaolin suspension and river water used for potable water.

EXPERIMENTAL

Materials

Exudate from *A. occidentale* trees (crude cashew gum) was supplied by the Brazilian company EMBRAPA (Empresa Brasileira de Pesquisa Agropecuária) from their experimental plantation in Fortaleza/Ceará. The crude gum was purified with sodium chloride solution before use according to the procedure described by Rodrigues *et al.*[32] Acrylamide (Aam) and potassium persulfate (KPS) supplied by Sigma-Aldrich and Vetec, respectively, were used as received. Kaolin colloidal precipitates (suspension zeta potential = −14.0 mV at pH 3.5) was supplied by CADAM S.A. and the commercial flocculant Flonex-9045 was donated by SNF Floerger. Raw river water and river water coagulated with aluminum sulfate were supplied by the Water and Sewers Department (DEMAE) of the Porto Alegre Prefecture.

Ultrasound Assisted Synthesis of Polyacrylamide Grafted Cashew Gum (CG-*g*-PAM)

The initiator KPS and ultrasound energy were used to generate free radical sites and to assist the polymerization of Aam on the polysaccharide backbone. In a 50 mL glass flask, one gram of CG (6.17 mmol of anhydroglucose unit) was dissolved in distilled water (15 mL) at room temperature. After, the required amount of the initiator KPS and acrylamide, dissolved previously in 2 mL and 13 mL of water, respectively, were added on the CG solution. The molar ratio between acrylamide and anhydroglucose unit (Aam:CG) and KPS amount are shown in Table I. After mixing, the solution was poured into a 100-mL three-neck round-bottom flask affixed with an ultrasound probe. The flask was sealed with a septum stopper and flushed with nitrogen gas for 20 min. The mixture was ultrasonicated using an ultrasonic generator (VCX 750, Sonics & Materials) with a 13 mm stainless steel sonic wave emission probe, operating at an output power of 750 W and a 20 kHz frequency. The actual

dissipation power of the probe was determined using a calorimetric method[33] and was 20.4 W at 30% amplitude. The temperature of the reactional medium increased spontaneously from room temperature to (70 ± 5) °C, during the sonication process that has taken 10.5 ± 1 min, until the solution has reached the gel point. The reaction was ended by immersing the flask in ice water bath. The cooled gel was poured into an excess of acetone, and the precipitate was collected and dried in an oven at 60 °C. The dried precipitate was pulverized and purified by solvent extraction with formamide and acetic acid (1:1 v/v) to remove the homopolymer.[34] PAM homopolymer was obtained under the same reaction conditions, with 0.190 mmol of initiator KPS and 30 mL of a 2 M Aam solution.

Control experiments without ultrasound energy were carried out in a thermostatic bath. Two solutions of CG (1 g, 6.17 mmol), Aam (6.57 g, 92.49 mmol) (Aam:CG molar ratio of 15:1), and KPS initiator (0.285 mmol) were prepared in 30 mL of distilled water and purged with nitrogen for 20 min. In the first experiment (CG-*g*-PAM-Control I) the temperature increased from room temperature to 56 °C, and the gel point was reached at 30 min, when the flask was immersed in ice-water bath to stop the reaction. In the second experiment (CG-*g*-PAM-Control II) the temperature was kept at 70 °C and the gel point was reached at 13 min.

The percentage of grafting (%*G*), grafting efficiency (%*E*) and percentage of conversion of acrylamide (%*C*) were evaluated according to Silva *et al.*,[7] as in the Eq. (1) to (3).

$$\%G = \frac{\text{mass of Aam in the graft copolymer}}{\text{mass of cashew gum}} \times 100 \quad (1)$$

$$\%E = \frac{\text{mass of graft copolymer}}{\text{mass of (cashew gum + acrylamide)}} \times 100 \quad (2)$$

$$\%C = \frac{\text{mass of acrylamide in the graft copolymer}}{\text{mass of acrylamide taken}} \times 100 \quad (3)$$

where the mass of Aam in the graft copolymer was calculated as mass of graft copolymer minus the mass of cashew gum taken. The %*E* describes the percentage of synthetic polymer that has been grafted onto the CG.

The percentage of grafting (%G') was also calculated in relation to the mass of graft copolymer as in the Eq. (4).

$$\%G' = \frac{\text{mass of Aam in the graft copolymer}}{\text{mass of graft copolymer}} \times 100 \quad (4)$$

Characterization

Intrinsic Viscosity Measurement. Viscosity measurements of the polymer solutions were carried out with an Ubbelohde viscometer (viscosity constant: 0.004925 (mm^2 s^{-2}); capillary diameter: 0.46 mm) at (25 ± 0.1) °C in a 0.1*M* NaCl aqueous solution. The time of flow for solutions was measured at five different concentrations (0.5, 0.2, 0.1, 0.05, and 0.025 g dL^{-1}). From the time of flow of polymer solutions (t) and that of the solvent (t_0, for 0.1*M* NaCl), relative viscosity ($\eta_{rel} = t/t_0$) was obtained. Subsequently, specific viscosity ($\eta_{sp} = \eta_{rel} - 1$), reduced viscosity ($\eta_{red} = \frac{\eta_{sp}}{C}$), and inherent viscosity ($\eta_{inh} = \frac{\ln \eta_{rel}}{C}$) were calculated, where '*C*' represents polymer concentration in g dL^{-1}. The intrinsic viscosity was obtained from the point of intersection after extrapolating of the plots of η_{red} and η_{inh} versus *C* to the zero concentration.[35]

Fourier Transform Infrared (FTIR) Spectroscopy. FTIR spectra of the CG, PAM, and grafted copolymers were recorded using KBr pellets in an FTIR spectrophotometer (Spectrum 1000, Perkin Elmer) between 400 and 4000 cm^{-1}.

Nuclear Magnetic Resonance (NMR) Spectroscopy. The ^{13}C NMR spectra of the CG, PAM, and graft copolymer (CG-*g*-PAM-6[190]) were recorded at 125 MHz using D_2O solutions at 50 °C, in an NMR spectrometer (DD2, Agilent 500-MHz) with standard pulse programs.

Thermal Analysis. Differential scanning calorimetry (DSC) thermograms of CG, PAM, and graft copolymers were obtained in a DSC calorimeter (Q20, TA Instruments) at a heating rate of 10 °C min^{-1} under nitrogen atmosphere (50 mL min^{-1}). The samples were first heated from 25 to 230 °C, cooled to 25 °C, and then re-heated to 230 °C.

Dynamic Light Scattering (DLS). The hydrodynamic radius (R_h) of GC, PAM, and graft copolymers was performed at 25 °C using a Brookhaven Instrument standard setup (BI-200 M goniometer, BI-9000AT digital correlator) with a He-Ne Laser ($\lambda = 632.8$ nm) as a light source. The autocorrelation functions of the scattered intensity were analyzed by the cumulant method. Solutions of CG (20 mg mL^{-1} in 0.1*M* NaCl), PAM, and graft copolymers (8 mg mL^{-1} in 0.1*M* NaCl) were prepared at 40 °C and ultracentrifuged (UniCen, Herolab) at 6000 rpm for 60 min, to eliminate any remaining insoluble particles. The value of the apparent R_h was determined by DLS at a 90° angle through the Stokes–Einstein equation [Eq. (5)], where k_B is the Boltzmann constant (1.38×10^{-23} J K^{-1}), *T* is the temperature system, η is the solvent viscosity, and *D* is the diffusion coefficient, calculated by the equipment itself.[36]

$$R_h = \frac{k_B T}{6\pi\eta D} \quad (5)$$

Performance Evaluation of the Flocculants

Flocculation Test Using Kaolin Suspension. Flocculation tests of kaolin suspension were carried out at ambient temperature (25 ± 2) °C using a Jar Test apparatus (JT-203, MILAN), equipped with six vases, which have stainless-steel paddle stirrer. Flocculation efficacy of CG-*g*-PAM was compared with those of the CG and the commercial flocculant, Flonex-9045 (based on Aam/sodium acrylate) using a standard test method. The kaolin suspension (0.3 g L^{-1} in distilled water) was adjusted to the desired pH by adding aqueous solution of HCl. The stock solutions of CG-*g*-PAM, CG, and Flonex-9045 in distilled water were prepared before the jar test procedure. Specific concentrations of the flocculants were added into each vase containing 1 L of kaolin suspension. The suspensions were stirred under identical conditions at 120 rpm for 30 s initially (to mix the flocculant and kaolin particles), followed by another 5 min of stirring at 60 rpm for flocs growth. The flocs were then left to settle for 9 min. At the end, the turbidity of the supernatant liquid was measured using a calibrated nephelometric turbidimeter (2100N, Hach).

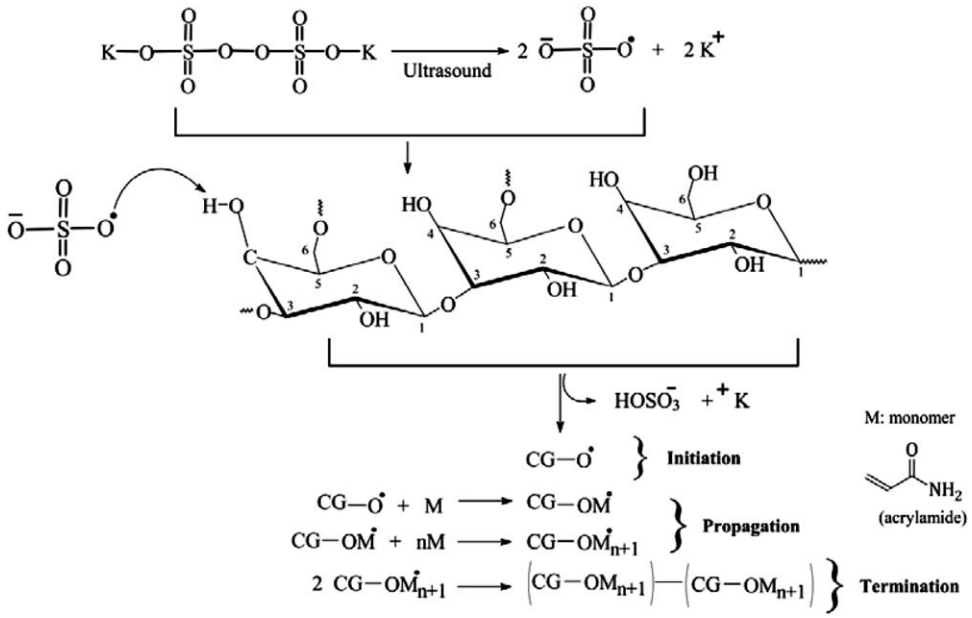

Figure 1. Mechanism of copolymerization of Aam/CG via an ultrasound assisted method.

Flocculation Test Using River Water. The flocculation efficacy of CG-*g*-PAM-15[285] (the best grade of PAM-grafted CG) was studied via a jar test procedure using raw river water (instead of a kaolin suspension solution) and compared to Flonex-9045 as well as aluminum sulfate, a coagulant commonly used in drinking water treatment. The water pH was adjusted to 2.0 with 1*M* HCl solution prior to the addition of the flocculant, as this has been shown to promote the CG copolymer-aided flocculation process. Specific volumes of the CG-*g*-PAM-15[285] and Flonex-9045 solutions were added into each vase containing the raw river water. The suspension was immediately stirred at 120 rpm for 5 min, followed by another 15 min at 60 rpm. After switching off the stirrer, the flocs were left to settle for 25 min. The quality of the supernatants (collected from the individual vases) was analyzed by standard turbidity and total suspended solid (TSS) procedures. The turbidity and TSS of raw water that has been treated with aluminum sulfate by the Water and Sewage Department was also analyzed.

RESULTS AND DISCUSSION

The characteristics and properties of the CG-*g*-PAM copolymers are reported in terms of (i) monomer and initiator concentrations, (ii) chemical modification of the CG, (iii) change in the intrinsic viscosity and thermal behavior of the copolymers, and (iv) flocculation performance of the CG-PAM copolymers in a kaolin suspension and raw river water for human consumption. Mechanism for the grafting reaction of Aam onto the CG backbone under ultrasound energy, and for flocculation process using CG-*g*-PAM copolymer with protonated amide nitrogen groups ($CONH_3^+$) and Flonex-9045 are proposed.

Synthesis of the CG-*g*-PAM Copolymers by an Ultrasound Assisted Method

The graft copolymers were obtaining by using the grafting-from method, in which the macromolecular backbone is chemically modified to introduce active sites capable of initiating functionality. The grafting copolymerization was ultrasound-assisted in aqueous medium aiming to increase the concentration of soluble radicals in the CG chain that are partly generated as a result of intense acoustic cavitation caused by the ultrasound energy.[37] In a blank reaction without the monomer Aam, the cashew gum under ultrasound energy has degraded, since no gel point was observed and the intrinsic viscosity of the fresh reagent solution was much higher than the sonicated solution after the reaction time. The mechanism of the PAM-CG backbone grafting reaction is depicted in Figure 1. The synergism between the initiator $K_2S_2O_8$ and the ultrasound energy has facilitated the sulfate anion radicals ($SO_4^{\bullet -}$) to abstract the hydrogen from the hydroxyl groups generating active sites or radicals on the CG backbone. The macro-radicals CG-O$^\bullet$ incorporate the Aam monomers onto the CG backbones to derive a graft copolymer.[38,39] Under ultrasound energy, the graft copolymer is more produced than the homopolymer. In the conventional reaction (CG-*g*-PAM-Control I), without ultrasound, the grafting efficiency %*E* was 79% and in the reaction with ultrasound (CG-*g*-PAM-15[285]) the %*E* was 94%. Using ultrasound, there was an increase of 15% in the grafting efficiency and a decrease from 21% to 6% of the homopolymer, besides a decrease in the reaction time from 30 to 10 min. Thus, the ultrasound favors hydrogen abstraction from the CG's hydroxyl groups by the sulfate anion radicals, disfavoring homopolymerization.

The ultrasound energy leads to high %*E* and high grafting number of PAM short-chain on the CG backbone. Unlike, in the conventional grafting reaction (CG-*g*-PAM-Control I), without ultrasound energy, only a low concentration of active site on the GC chains is favored, leading to a low %*E* and low grafting number of PAM long-chain on the CG backbone. The use of ultrasound for modifying CG is an effective alternative to produce graft copolymers, since it generates radicals preferably on the CG backbone due to the cavitation process. The

emergence of new technologies using alternative forms of energy (e.g., ultrasound and microwave), together with a renewed interest in biopolymer-based flocculants, will lead to cleaner and more energy efficient chemical processes in the future.

Table I shows the values of percentage of grafting (%*G*), grafting efficiency (%*E*), percentage of conversion of acrylamide (%*C*), intrinsic viscosity (η), and hydrodynamic radius (R_H) of (i) the synthesized CG-*g*-PAM copolymers, obtained at different monomer (Aam) and initiator (KPS) concentrations, (ii) the PAM homopolymer obtained in the absence of CG, and (iii) the pristine CG. The reaction mixture was continuously ultrasonic-irradiated under a nitrogen atmosphere until it reached the gel point or changes in the solution viscosity were observed. The average reaction time of the grafting copolymerization at the Aam and KPS concentrations evaluated was approximately 10 min. It is shorter than the conventional reaction at the same condition but without ultrasound energy that has taken 30 min, and the reaction time of experiments reported by Silva *et al.*[7] of 180 min. The advantage of using ultrasound instead of microwave energy in chemical reactions is that the latter increases the temperature quickly in a short period of time resulting in an intermittent process, whereas with the former, or sonication process, the temperature increases continuously with high conversion at the end of reaction.

Monomer Concentration. With the increase in the monomer concentration the %*G* and %*G*′ increased continuously, corroborating the data reported by Silva *et al.*[7] As the concentration of Aam was increased, %*E* and %*C* rose gradually and achieved the maximum value when the molar ratio Aam to CG was 15:1. Higher value of Aam:CG molar ratio (20:1) and 0.190 mmol of KPS did not affect the %*E* and %*C*. High grafting efficiency (>90%) at the Aam:CG molar ratio of 15:1 corresponded to a low fraction of homopolymer. Similar results have been reported for the grafting of Aam onto chitosan[15] and Kundoor mucilage.[40] A high monomer concentration provides more Aam molecules per polysaccharide macroradical, leading to a higher %*E*[41], and any decrease in the %*E* is due to the preferential occurrence of homopolymerization over graft copolymerization.

The CG-*g*-PAM-Control I copolymer prepared by conventional method (reaction time of 30 min) presented values of %*G*, %*E*, and %*C* lower than those of the copolymer CG-*g*-PAM-10^{285} synthetized by using ultrasound (reaction time of 10 min) (Table I). The cavitation process increases the concentration of radical active sites onto CG chains and facilitates monomer diffusion in the reaction medium, consequently, increasing the %*E* and %*C*. On the other hand, in the conventional method there is low active sites concentration onto CG chains and the homopolymerization is facilitated.

The intrinsic viscosity of the graft copolymers changes from 1.0 and 2.7 dL g^{-1}, being much higher than the CG viscosity of 0.12 dL g^{-1}. The PAM homopolymer and graft copolymer obtained at the Aam to CG molar ratio of 20:1 and a KPS amount of 0.190 mmol both had an intrinsic viscosity value of 3.5 dL g^{-1}. High viscosity hinders the movement of free radicals and monomer molecules, resulting in the increase of chain transfer to the monomer molecules.[42,43] The copolymers CG-*g*-PAM-Control I and CG-*g*-PAM-Control II, obtained by conventional method, presented intrinsic viscosity higher than that of the CG-*g*-PAM copolymers prepared with ultrasound energy (Table I). The intrinsic viscosity of the CG-*g*-PAM copolymers depends on the number and length of the grafting of PAM incorporated in the CG chains. In absence of ultrasound energy the %*E* is low and the PAM grafting onto CG backbone is longer since the relation monomer/active site concentration is lower than in the reaction under ultrasound energy. As larger the length and lower quantity of the grafting, higher will be the chains entanglement and thus the viscosity.

Initiator Concentration. At the lowest Aam to CG molar ratio of 6:1, increasing the initiator quantity from 0.190 to 0.380 mmol increased the %*E*, from 55% (CG-*g*-PAM-6^{190}) to 71% (CG-*g*-PAM-6^{380}). Elevating the initiator concentration increases the active radical sites on the CG, and this directly aids the monomer conversion. Copolymers synthesized at the Aam to CG molar ratio of 10:1 and 15:1 was not influenced by the initiator concentration used and the %*E* obtained was around 80% and 90%, respectively. However, graft copolymers that were obtained using the highest KPS concentration showed, in general, the lowest intrinsic viscosity and hydrodynamic radius values. The chain branching length decreased with an increasing initiator concentration owing to the higher probability of finding the CG-O$^{\bullet}$ radicals on the CG skeleton. The number and length of the long chain branching directly affect the polymer structure and consequently, its hydrodynamic radius. For a given monomer concentration, a high initiator concentration generates a larger number of short PAM chains, which are then grafted onto the CG backbone. Therefore, in solution, the chain coil of the graft copolymer would not expand much more than the CG chain. As pointed out by Lanthong *et al.*,[44] kinetic chain length decreases with an increasing initiator concentration, which in turn directly affects the molecular weight of the polymer, resulting in low hydrodynamic radius and intrinsic viscosity value. On the other hand, at a low initiator concentration, a smaller number of long PAM chains are grafted onto the CG backbone. In this case, the compact shape of the CG coil will expand owing to the presence of long chain branching.[45] This would result in a larger hydrodynamic radius (>250 nm) compared with the radius of the gum, as observed in our work, leading to higher intrinsic viscosities. The hydrodynamic radius is the effective cross-sectional diameter of a polymeric chain in solution. The diameter detection limit of the instrument used is between 2 and 500 nm. For graft copolymers with an effective diameter that is significantly higher than the limit of the instrument, their hydrodynamic radius values were taken as being higher than the maximum value (250 nm) that could be measured.

Chemical Modification of the Cashew Gum

The insertion of PAM grafting onto the CG backbone was confirmed by comparing the FTIR spectra of the graft copolymer (CG-*g*-PAM-15^{190}) to that of pure CG, as shown in Figure 2. The FTIR spectrum of the CG displays a broad peak at 3384 cm^{-1} because of the stretching vibrations of O−H, and a shoulder at 2932 cm^{-1} assigned to the C−H symmetrical and asymmetrical stretching vibrations. The absorption band at

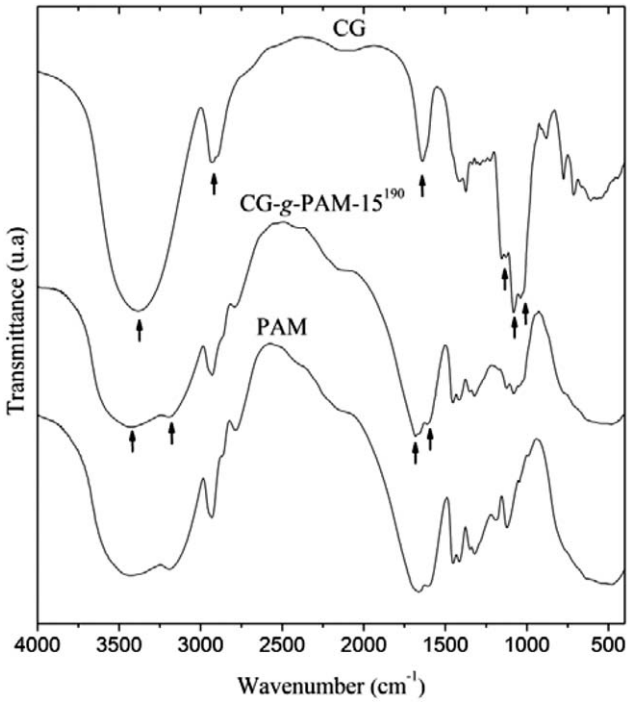

Figure 2. FTIR spectra of CG, CG-*g*-PAM-15[190], and PAM.

1639 cm^{-1} is attributed to the O−H scissor vibrations from bonded water molecules. Strong absorption peaks at 1153, 1081, and 1038 cm^{-1} are assigned to the stretching vibrations of C−O−C from glucosidic linkages.[46] Meanwhile, the FTIR spectrum of CG-*g*-PAM-15[190] exhibits a sharp absorption peak at 1650 cm^{-1} and a shoulder at 1607 cm^{-1}, attributed to the C=O (primary amide) stretching and the NH_2 scissor vibrations of PAM, respectively. The strong absorption at 3432 cm^{-1} and the shoulder at around 3206 cm^{-1} are attributed to N–H stretching. The presence of the N−H and C=O stretching vibrations in the graft copolymer confirms the successful grafting reaction of Aam moieties onto the CG backbone.

The ^{13}C NMR spectra of CG, CG-*g*-PAM-6[190], and PAM are shown in Figure 3. The ^{13}C NMR spectrum of CG has three distinct resonance signals. The peak in the range of 95-110 ppm is attributed to the anomeric carbon atom. The absorption peaks at 59-63 ppm are assigned to the carbon of the CH_2OH group, located at C-6. The overlapping peaks in the range of 65-85 ppm are assigned to carbon atoms with –OH groups (C-2, C-3, C-4, and C-5) of the pyranose ring. The small peak at 16.8 ppm is attributed to CH_3 of rhamnose. These signals are in accordance with previous studies.[30] Meanwhile, the ^{13}C NMR spectrum of PAM has a peak at 179.7 ppm owing to the amide carbonyl carbon (C=O). NMR peaks in the regions of 33–37 ppm and 41–43 ppm are assigned to the CH_2 and CH groups, respectively. The small peak at 130 ppm is an indication of the residual monomer of Aam. The ^{13}C NMR spectrum of CG-*g*-PAM-6[190], in contrast to the CG spectrum, displays an intense peak at 179.7 ppm owing to the carbonyl groups, along with two additional peaks at 35 and 42 ppm, which are attributed to the methylene groups and the carbon connected to the carbonyl group, respectively. The NMR spectra agree with the results obtained via the FTIR analysis. The ^1H NMR spectrum of CG-*g*-PAM-6[190], when compared to that of the unmodified CG, shows two additional peaks at 1.5–2.0 ppm and 2.2–2.5 ppm, resulting from the PAM protons of the branching chain grafted onto the CG backbone.

Estimation and Interpretation of Intrinsic Viscosity

It is well known that a polymer's intrinsic viscosity is a measure of its hydrodynamic volume in solution, which in turn is a function of the molecular weight and structure of the molecules, and it depends on the nature of the solvent and temperature.[35] The CG used in this study has an intrinsic viscosity of 0.12 dL g^{-1} (Table I), and has a highly branched architecture owing to a large proportion of end-groups such as rhamnose, xylose, mannose, glucose, arabinofuranose, arabinopyranose, galactose, and glucuronic acid in its structure.[47] The CG's intrinsic viscosity in a 0.1*M* NaCl aqueous solution is in line with data reported in the literature.[7,30] The PAM homopolymer synthesized for this study showed intrinsic viscosity thirty times higher than the CG, as a result of its longer linear chain. The intrinsic viscosity of the graft copolymers is higher compared with the, CG owing to the PAM grafting on the polysaccharide chains (which resulted in a higher molecular weight), but is lower when compared with the PAM. For CG-*g*-PAM-6 and CG-*g*-PAM-10, their intrinsic viscosities are inversely proportional to the initiator concentration, as described previously. However, the intrinsic viscosity of CG-*g*-PAM-15 increased, owing to either a higher Aam concentration or longer chain branching. Thus, lower initiator and higher monomer concentrations, each resulted in the increase of the intrinsic viscosity and length of the grafted chains. According to the Mark–Houwink–Sakurada relationship ($\eta = KM^{\alpha}$),[35] the constants K and α depend on the polymer type, solvent, and temperature, and the intrinsic viscosity (η) is proportional to the molar mass (M) of the polymer molecules. Thus, an increase in the intrinsic viscosity is a direct consequence of a higher polymer molecular weight. The molecular weight increase can be attributed to either an extension of the linear chain or the formation of more branched chains with varying branching length. Based on the proposed reaction mechanism and the differences in the intrinsic viscosities of the graft copolymer (compared to the pristine CG), we postulated that the graft copolymer reaches a considerable volume in aqueous solution and is appropriate for use as a flocculant.

Thermal Evaluation of the CG-*g*-PAM Copolymers

The first (a) and second (b) heating DSC curves of CG-*g*-PAM-10[190], CG, and PAM are shown in Figure 4. The CG's first heating curve has an endothermic peak at approximately 125 °C due to the evaporation of adsorbed and linked water. The reheating of the CG did not show any events that suggest the amorphous nature of the polysaccharide.[48] The PAM's first heating curve shows two endothermic events at 118 and 185 °C, with the former assigned to water evaporation due to the sample's absorbed moisture. Meanwhile, the PAM's second heating curve shows only the latter event that corresponds to a thermal event with mass loss, also detected by thermogravimetric analysis in the same temperature range. The event at approximately 185 °C is because of the oxidation and cycling of the chain, involving the

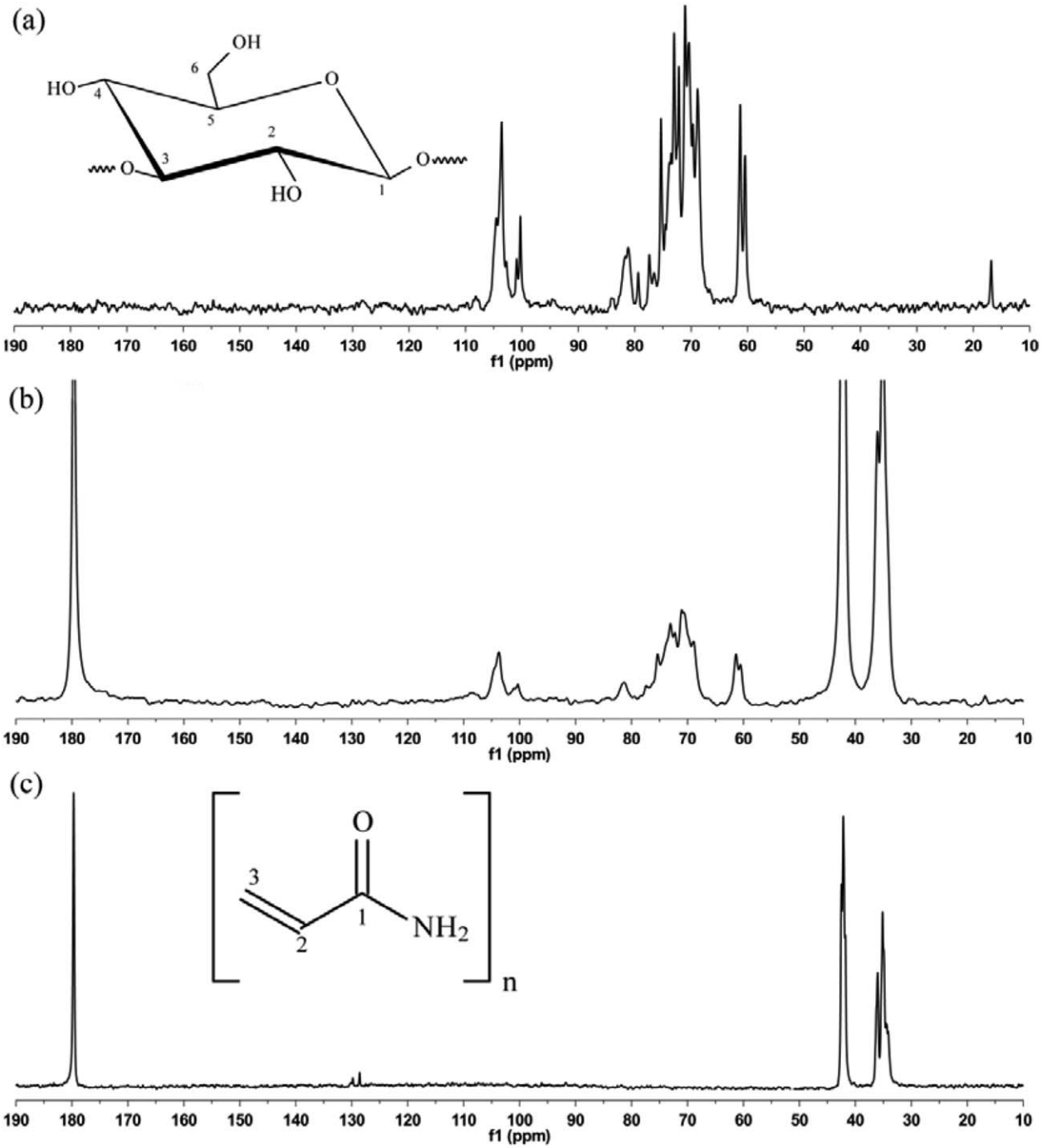

Figure 3. ^{13}C NMR spectra of CG (a), CG-*g*-PAM-6[190] (b), and PAM (c).

amide groups that undergo carbonization,[49] since the residue content was measured at 14% under a nitrogen atmosphere. The PAM homopolymer obtained in this study was amorphous owing to its distinct polymerization mechanism and process, as opposed to the results of Biswal and Singh[11] and Silva *et al.*,[7] in which both have reported an endothermic event at 203 °C attributed to the melting point of the polymer. The glass transition temperature (T_g) can be better observed in the second DSC run at 187 °C, as reported in the literature.[50] The copolymer, CG-*g*-PAM-10[190], has a similar DSC curve profile to the PAM homopolymer. The lower T_g of the grafted copolymer (175 °C) is because of the shorter PAM chains that were grafted onto the CG backbone, compared with the linear, high molecular weight PAM homopolymer.

Flocculation Performance of the CG-*g*-PAM Copolymers

Effect of pH and Flocculant Content on the Turbidity of Kaolin Suspension. A pH value in the range of 2.0−3.5 decreased the turbidity of the kaolin suspension, when flocculated with CG-*g*-PAM, and a pH of 4.0 onwards resulted in the

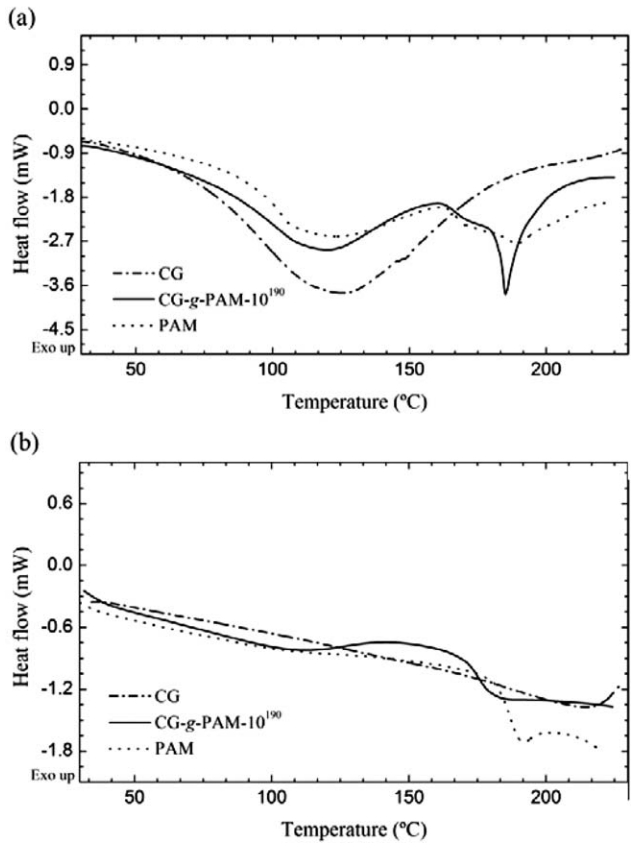

Figure 4. DSC curves of CG, CG-*g*-PAM-10^{190}, and PAM. (a) 1st and (b) 2nd heating run.

increase of turbidity. The supernatant became cleaner and more transparent, after sedimentation of 9 min, whereas the turbidity value declined from 432 to less than 10 NTU at pH 3.5. The observed turbidity improvement between pH 2 and 3.5 may be attributed to a better flocculation process of the kaolin particles. The protonation process takes place at pH under 4.0, at which the $CONH_2$ moieties are converted to $CONH_3^+$.[51] The protonation of the amide nitrogen under acidic conditions enhances the interaction between these cations and the negatively charged kaolin particles in suspension, hence creating bigger agglomerates or floccules. The destabilization of kaolin suspension is due to a charge neutralization that reduces the potential energy of repulsion between adjacent colloidal particles. The flocculant adopts a rather flat adsorbed configuration and in this state, its action occurs mainly through electrostatic patch interactions.

Figure 5 shows the turbidity removal of the kaolin suspension as a function of the flocculant type and concentration at pH 3.5. The flocculation efficacy of almost all CG-*g*-PAM graft copolymers were higher than 90%, with the exception of CG-*g*-PAM-6^{380} and CG-*g*-PAM-10^{380}, which showed poor performance because of shorter chain branching associated with the polymer grafts and lower hydrodynamic radius. On the other hand, graft copolymers with hydrodynamic radius larger than 250 nm, as well as containing fewer and longer PAM grafted chains, have shown maximum flocculation efficacy. A good correlation between the flocculation efficacy and the graft copolymers' percentage of grafting and intrinsic viscosity was observed (Table I). Among the various CG-*g*-PAM graft copolymers, CG-*g*-PAM-10^{285} showed the maximum flocculation efficacy by reducing approximately 96% of the kaolin suspension's turbidity, at a dosage of 1.0 mg/L.

The performance of CG-*g*-PAM-10^{285} and Flonex-9045 was similar, with a turbidity removal of approximately 96%, at respective dosages of 1.0 and 1.25 mg/L. Although the efficiency of the graft copolymer and the commercial flocculant in terms of turbidity removal was comparable, there were noticeable differences in the size and shape of flocs after 9 min of sedimentation. The flocs produced using Flonex-9045 were bigger and heavier than those obtained with CG-*g*-PAM-15^{285}. This could be explained in terms of the structural and conformational differences of the polymer chains in aqueous solution. Flonex-9045 is an anionic linear Aam and sodium acrylate copolymer and its chains exist in the more extended forms in solution. Figure 6 shows a comparison between two proposed flocculation mechanisms of kaolin using either Flonex-9045 or CG-*g*-PAM as the flocculant.

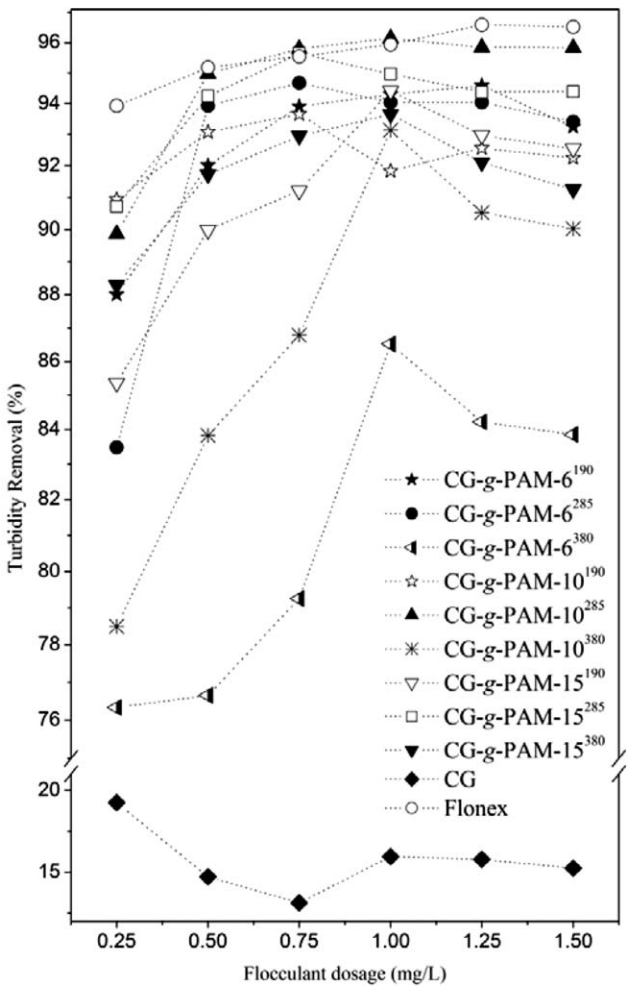

Figure 5. Turbidity removal of kaolin suspension as a function of the flocculant concentration and type.

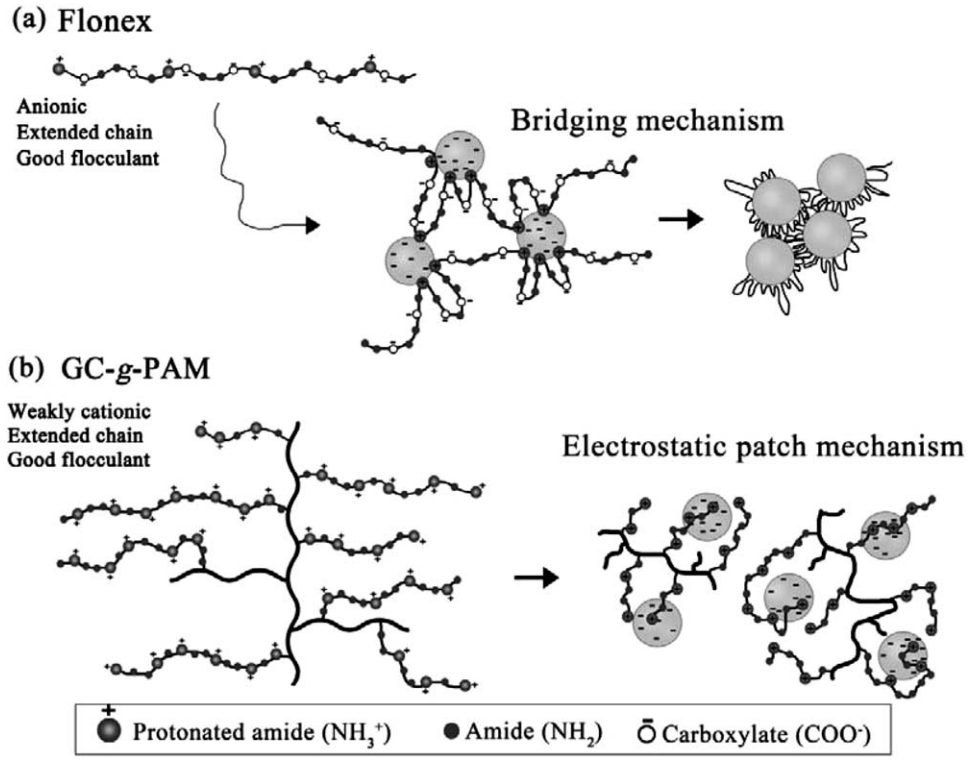

Figure 6. Proposed flocculation mechanisms of kaolin: bridging mechanism with Flonex 9045 (a), versus charge neutralization or patch mechanism with CG-*g*-PAM (b).

The larger floc size obtained using Flonex-9045 corroborates the polymer bridging mechanism.[52] The presence of the nonionic amide and ionic acrylate groups maximizes the aggregation process, indicating clearly that the ionic acrylate groups are predominantly responsible for the polymer chain extension of the macromolecules, without themselves playing a direct role in the flocculation mechanism.[53] Thus, the adsorption on the kaolin particles occurs by virtue of the protonated amide nitrogen groups ($CONH_3^+$) present in the Aam units. On the other hand, the high flocculation efficiency with the CG-*g*-PAM-15^{285} graft copolymer should be initially attributed to the branched structure of the CG, with the PAM grafts subsequently extending and opening the CG chain in solution. The rigidity of the interring linkages of polysaccharide in solution is akin to fairly stiff extended rods. This kind of CG molecular configuration in solution, probably favors the expansion of the PAM branches and thus, of the protonated amide nitrogen groups ($CONH_3^+$). Furthermore, the higher the cationic charge density (as a function of protonated amide nitrogen groups), the greater the intramolecular repulsion between equal-sign charges on the PAM grafts. The formation of flocs with smaller dimensions than those obtained using the long chain anionic Flonex-9045 is related to the electrostatic patch mechanism, caused by the attractive forces between the highly negative kaolin particles and the protonated amide nitrogen groups. According to Angle *et al.*,[54] the charge patch mechanism usually produces relatively small flocs with slow settling rates. This result suggests that the cationic chains of CG-*g*-PAM-15^{285} adsorb onto particle surfaces, in a flat configuration, owing to a strong electrostatic attraction and the poor bridging ability of the copolymer.

Turbidity of River Water Suspension versus the Flocculant Type. The quality indices of river water treated with 0.5 mg/L of CG-*g*-PAM-15^{285} and Flonex 9045, as well as of river water treated with aluminum sulfate by the Water and Sewers Department (DEMAE), are reported in Table II. CG-*g*-PAM-15^{285} proved highly effective in pollutant load removal from the river water. After a settling time of 25 min, the turbidity and TSS

Table II. Removal of the Turbidity and TSS of River Water by Using the Flocculants CG-*g*-PAM-15^{285} or Flonex-9045, or Aluminum Sulfate

Flocculant	pH (–)	Flocculant (mg L^{-1})	TSS (mg L^{-1})	Turbidity (NTU)	Turbidity removal (%)
Raw river water	7.3	—	127 ± 17	35.67 ± 1.25	—
CG-*g*-PAM-15^{285}	2.0	0.5	97 ± 29	3.25 ± 0.25	90.9
Flonex	2.0	0.5	73 ± 25	3.20 ± 0.20	91
$Al_2(SO_4)_3$	6.1	—	47 ± 9	2.34 ± 0.02	93.4

removal values were 90.9% and 24%, respectively. A comparative study between CG-*g*-PAM-15^{285} and Flonex-9045 showed similar results, within experimental error. Nonetheless, aluminum sulfate did show a better pollutant load reduction ability compared with CG-*g*-PAM-15^{285} and Flonex-9045, with the values of 93.4% and 63% for turbidity and TSS removal, respectively. The high coagulation efficiency with aluminum sulfate should therefore be attributed to the high dosage of coagulant used, which can vary from 7 to 17 mg/L as reported by Yang *et al.*[55]

As discussed, the main concern of using an inorganic and synthetic coagulant is the possible link between residual aluminum in treated water and Alzheimer's disease, as well as the health risks associated with unreacted monomers (i.e., Aam), which could produce severe neurotoxic effects.[27,28] As such, the CG-*g*-PAM copolymer can be used as a substitute for inorganic and synthetic flocculants in water treatment plants owing to its biodegradability and wide availability (from sustainable plantation or forest resources).

CONCLUSIONS

The use of an ultrasound assisted method for the PAM –based modification of CG not only reduces the graft copolymerization time but also promotes high grafting efficiency. The use of low frequency ultrasound waves at room temperature has proved to be an effective and simple method in assisting graft polymerization reaction with higher conversion. CG-*g*-PAM copolymers with high grafting efficiency (%*E*) and higher intrinsic viscosity than the pristine polymer were obtained using Aam to CG molar ratio of 15:1. Low initiator concentrations generated a small number of PAM long chain grafted on the CG backbone and vice-versa. CG-*g*-PAM copolymers with the highest hydrodynamic radius showed the maximum flocculation efficacy, and it can be applied as a substitute for commercial PAM-based flocculants (e.g., Flonex 9045). For the CG-*g*-PAM copolymers, the electrostatic patching mechanism predominates, as opposed to the bridging mechanism for Flonex 9045, as a result of the protonated amide nitrogen groups ($CONH_3^+$) present in the PAM chains. The slight cationic character of CG-*g*-PAM favors electrostatic-induced adsorption on negative surfaces, making it an efficient flocculant. The CG-*g*-PAM-15^{285} flocculant has shown a good performance in the reduction of total pollutant, and can be used as a substitute for inorganic coagulant (e.g., aluminum sulfate) in river water treatment. In conclusion, this study demonstrated that CG-grafted-PAM copolymers are a promising material to be developed as high performance flocculant for the treatment of potable water as well as wastewater. In addition, the current form of the CG-*g*-PAM copolymer can be used as a fundamental template for the design of other flocculants.

ACKNOWLEDGMENTS

The authors gratefully acknowledge the financial support from CNPq and CNPCa-EMBRAPA for cashew gum supply.

REFERENCES

1. Kumar, K.; Adhikary, P.; Karmakar, N. C.; Gupta, S.; Singh, R. P.; Krishnamoorthi, S. *Carbohydr. Polym.* **2015**, *127*, 275.
2. Rana, V.; Rai, P.; Tiwary, A. K.; Singh, R. S.; Kennedy, J. F.; Knill, C. J. *Carbohydr. Polym.* **2011**, *83*, 1031.
3. Singh, V.; Kumar, P.; Sanghi, R. *Prog. Polym. Sci.* **2012**, *37*, 340.
4. Wunderlich, T.; Stelter, M.; Tripathy, T.; Nayak, B. R.; Brenn, G.; Yarin, A. L.; Singh, R. P.; Brunn, P. O.; Durst, F. *J. Appl. Polym. Sci.* **2000**, *77*, 3200.
5. Toti, U. S.; Soppimath, K. S.; Mallikarjuna, N. N.; Aminabhavi, T. M. *J. Appl. Polym. Sci.* **2004**, *93*, 2245.
6. Wang, T.; Nie, J.; Yang, D. *Carbohydr. Polym.* **2012**, *90*, 1428.
7. Silva, D. A.; Paula, R. C. M.; Feitosa, J. P. A. *Eur. Polym. J.* **2007**, *43*, 2620.
8. Rahul, R.; Jha, U.; Sen, G.; Mishra, S. *Carbohydr. Polym.* **2014**, *99*, 11.
9. Sen, G.; Kumar, R.; Ghosh, S.; Pal, S. *Carbohydr. Polym.* **2009**, *77*, 822.
10. Xie, C.; Feng, Y.; Cao, W.; Teng, H.; Li, J.; Lu, Z. *J. Appl. Polym. Sci.* **2009**, *111*, 2527.
11. Biswal, D. R.; Singh, R. P. *J. Appl. Polym. Sci.* **2004**, *94*, 1480.
12. Pandey, V. S.; Verma, S. K.; Yadav, M.; Behari, K. *Carbohydr. Polym.* **2014**, *99*, 284.
13. Rani, P.; Mishra, S.; Sen, G. *Carbohydr. Polym.* **2013**, *91*, 686.
14. Singh, V.; Tiwari, A.; Tripathi, D. N.; Sanghi, R. *Carbohydr. Polym.* **2004**, *58*, 1.
15. Wang, J.-P.; Chen, Y.-Z.; Zhang, S.-J.; Yu, H.-Q. *Bioresour. Technol.* **2008**, *99*, 3397.
16. Vahdat, A.; Bahrami, H.; Ansari, N.; Ziaie, F. *Radiat. Phys. Chem.* **2007**, *76*, 787.
17. Bera, S.; Mondal, D.; Martin, J. T.; Singh, M. *Carbohydr. Res.* **2015**, *410*, 15.
18. Bhanvase, B. A.; Pinjari, D. V.; Sonawane, S. H.; Gogate, P. R.; Pandit, A. B. *Ultrason. Sonochem.* **2012**, *19*, 97.
19. Prasad, K.; Sonawane, S.; Zhou, M.; Ashokkumar, M. *Chem. Eng. J.* **2013**, *219*, 254.
20. Lancaster, M. Green Chemistry: An Introduction Text; Royal Society of Chemistry: Cambridge, **2002**; p 210.
21. Mason, T. J.; Bernal, V. S. In Power Ultrasound in Electrochemistry: From Versatile Laboratory Tool to Engineering Solution; Pollet, B. Ed.; Wiley: United Kingdom, **2012**; Chapter 1, p 21.
22. Kardos, N.; Luche, J.-L. *Carbohydr. Res.* **2001**, *332*, 115. Available at: http://www.ncbi.nlm.nih.gov/pubmed/11434369.
23. Cheung, M. H.; Gaddam, K. *J. Appl. Polym. Sci.* **2000**, *76*, 101.
24. Pollet, B. G. *Int. J. Hydrogen Energy* **2010**, *35*, 11986.
25. Yan, Y.; Glover, S. M.; Jameson, G. J.; Biggs, S. *Int. J. Miner. Process.* **2004**, *73*, 161.

26. Bolto, B.; Gregory, J. *Water Res.* **2007**, *41*, 2301.
27. Rice, J. M. *Mutat. Res.* **2005**, *580*, 3.
28. Rondeau, V.; Commenges, D.; Jacqmin-gadda, H.; Dartigues, J. *Am. J. Epidemiol.* **2000**, *152*, 59.
29. Mothe, C. G.; Rao, M. A. *Thermochim. Acta* **2000**, *357358*, 9.
30. Paula, R. C. M.; Heatley, F.; Budd, P. M. *Polym. Int.* **1998**, *45*, 27.
31. Giri, T. K.; Pure, S.; Tripathi, D. K. *Polímeros Ciência e Tecnol.* **2015**, *25*, 168.
32. Rodrigues, J. F.; Paula, R. C. M.; Costa, S. M. O. *Polímeros Ciência e Tecnol.* **1993**, *3*, 31.
33. Margulis, M. A.; Margulis, I. M. *Ultrason. Sonochem.* **2003**, *10*, 343.
34. Fanta, G. F. In Block and Graft Copolymerization; Ceresa, R. J., Ed.; John Wiley & Sons: London, **1973**; Chapter 1, p 1.
35. Sperling, L. H. Introduction to Physical Polymer Science, 4th ed. Wiley: Hoboken, New Jersey.
36. Peres, G. L.; Leite, D. C.; Silveira, N. P. *Starch-Stärke* **2015**, *67*, 407.
37. Price, G. J.; Clifton, A. A. *Polymer* **1996**, *37*, 3971.
38. Pourjavadi, A.; Harzandi, A. M.; Hosseinzadeh, H. *Eur. Polym. J.* **2004**, *40*, 1363.
39. Sadeghi, M.; Mohammadinasab, E.; Shafie, F. *Sci. Res. Essays* **2012**, *7*, 511.
40. Mishra, A.; Bajpai, M. *J. Appl. Polym. Sci.* **2005**, *98*, 1186.
41. Wang, J.; Chen, Y.; Ge, X.; Yu, H. *Chemosphere* **2007**, *66*, 1752.
42. Eldin, M. S. M.; El-Sherif, H. M.; Soliman, E. A.; Elzatahry, A. A.; Omer, A. M. *J. Appl. Polym. Sci.* **2011**, *122*, 469.
43. Gupta, K. C.; Sahoo, S.; Khandekar, K. *Biomacromolecules* **2002**, *3*, 1087.
44. Lanthong, P.; Nuisin, R.; Kiatkamjornwong, S. *Carbohydr. Polym.* **2006**, *66*, 229.
45. Pal, S.; Nasim, T.; Patra, A.; Ghosh, S.; Panda, A. B. *Int. J. Biol. Macromol.* **2010**, *47*, 623.
46. Guilherme, M. R.; Campese, G. M.; Radovanovic, E.; Rubira, A. F.; Feitosa, J. P. A.; Muniz, E. C. *Polymers* **2005**, *46*, 7867.
47. Anderson, D. M.; Bell, P. *Anal. Chim. Acta* **1975**, *79*, 185.
48. Okoye, E. I.; Onyekweli, A. O.; Kunle, O. O. *Res. J. Appl. Sci. Eng. Technol.* **2012**, *4*, 3709.
49. Dyke, J. D. V.; Kasperski, K. L. *J. Polym. Sci. Part A: Polym. Chem.* **1993**, *31*, 1807.
50. Mahdavian, A.-R.; Zandi, M. *J. Appl. Polym. Sci.* **2003**, *87*, 2335.
51. Mahdavinia, G.; Pourjavadi, A.; Hosseinzadeh, H.; Zohuriaan, M. *Eur. Polym. J.* **2004**, *40*, 1399.
52. Sabah, E.; Cengiz, I. *Water Res.* **2004**, *38*, 1542.
53. Michaels, A. S. *Ind. Eng. Chem.* **1954**, *46*, 1485.
54. Angle, C. W.; Smith-Palmer, T.; Wentzell, B. R. *J. Appl. Polym. Sci.* **1997**, *64*, 783.
55. Yang, Z.; Gao, B.; Yue, Q. *Chem. Eng. J.* **2010**, *165*, 122.

SGML and CITI Use Only
DO NOT PRINT